Inorg. Chem. **2007**, *46*, 801–808

Single-Crystal Growth and Characterization of Disilver(I) Monofluorophosphate(V), Ag_2PO_3F: Crystal Structure, Thermal Behavior, Vibrational Spectroscopy, and Solid-State ^{19}F, ^{31}P, and ^{109}Ag MAS NMR Spectroscopy

Matthias Weil,*,† Michael Puchberger,‡ Ekkehard Füglein,§ Enrique J. Baran,|| Julia Vannahme,⊥ Hans J. Jakobsen,# and Jørgen Skibsted#

Institute for Chemical Technologies and Analytics, Division of Structural Chemistry, Vienna University of Technology, Getreidemarkt 9/164-SC, A-1060 Vienna, Austria, Institute of Materials Chemistry, Vienna University of Technology, Getreidemarkt 9/165-MC, A-1060 Vienna, Austria, Netzsch-Gerätebau GmbH, Wittelsbacher Strasse 42, D-95100 Selb, Germany, Centro de Química Inorgánica (CEQUINOR/CONICET, UNLP), Facultad de Ciencias Exactas, Universidad Nacional de La Plata, C. Correo 962, 1900-La Plata, Argentina, Institut für Physikalische Chemie, Westfälische Wilhelms-Universität Münster, Corrensstrasse 30, D-48149 Münster, Germany, and Instrument Centre for Solid-State NMR Spectroscopy, Department of Chemistry, University of Aarhus, Langelandsgade 140, DK-8000 Aarhus C, Denmark

Received September 18, 2006

Single crystals of disilver(I) monofluorophosphate(V), Ag_2PO_3F (**1**), were obtained by slow evaporation of a diluted aqueous Ag_2PO_3F solution. Compound **1** adopts a new structure type and crystallizes in the monoclinic space group $C2/c$ with eight formula units and lattice parameters of $a = 9.2456(8)$ Å, $b = 5.5854(5)$ Å, $c = 14.7840(13)$ Å, and $\beta = 90.178(2)°$. The crystal structure of **1** [$R(F^2 > 2\sigma(F^2)) = 0.0268$, $wR(F^2$ all$) = 0.0665$] is composed of three crystallographically independent Ag^+ cations and PO_3F^{2-} anions as single building units. The oxygen environment around each of the Ag^+ cations is different, with one Ag^+ in distorted octahedral ($\bar{d}$(Ag–O) = 2.553 Å), one in nearly rectangular ($\bar{d}$(Ag–O) = 2.445 Å), and one in distorted tetrahedral ($\bar{d}$(Ag–O) = 2.399 Å) coordination. Additional Ag–F contacts to more remote F atoms located at distances >2.80 Å augment the coordination polyhedra for the two latter Ag^+ cations. The monofluorophosphate anion deviates slightly from C_{3v} symmetry and exhibits the characteristic differences in bond lengths, with a mean of 1.510 Å for the P–O bonds and one considerably longer P–F bond of 1.575(2) Å. Compound **1** was further characterized by vibrational spectroscopy (Raman and IR) and solid-state ^{19}F, ^{31}P, and ^{109}Ag MAS NMR spectroscopy. The value for the isotropic one-bond P–F coupling constant in **1** is $^1J_{PF} = -1045$ Hz. Thermal analysis (TG, DSC) revealed a reversible phase transition at 308 °C, which is very close to the decomposition range of **1**. Under release of POF_3, $Ag_4P_2O_7$ and Ag_3PO_4 are the thermal decomposition products at temperatures above 450 °C.

Introduction

Inorganic monofluorophosphates(V), $M^I_2PO_3F{\cdot}xH_2O$ and $M^{II}PO_3F{\cdot}xH_2O$,[1] are important materials used as toothpaste additives,[2] wood preservatives,[3] corrosion inhibitors,[4] solubility inhibitors for lead in potable water sources,[5] and as active agents against osteoporosis or caries during biomineralization of fluoroapatite.[6] Therefore, much effort has been paid in the past to the preparation and structural characterization of these compounds. Possible preparation routes for monofluorophosphates include solid-state reactions between metal

* To whom correspondence should be addressed. Email: mweil@mail.zserv.tuwien.ac.at. Phone: ++43-1-58801-17122. Fax: ++43-1-58801-17199.

† Institute for Chemical Technologies and Analytics, Vienna University of Technology.

‡ Institute of Materials Chemistry, Vienna University of Technology.

§ Netzsch-Gerätebau GmbH.

|| Centro de Química Inorgánica, Universidad Nacional de La Plata.

⊥ Institut für Physikalische Chemie, Westfälische Wilhelms-Universität Münster.

Instrument Centre for Solid-State NMR Spectroscopy, University of Aarhus.

(1) In these compounds, M^I is an alkali metal or NH_4^+, and M^{II} is an alkaline earth metal, a first row transition metal, or tin; the water content x can range from 0 to 5.

(2) Ericsson, S. Y. U.S. Patent 3,119,743, Jan. 28, 1964.

(3) Möwius, F.; Meisel, M.; Grunze, H.; Kolditz, L.; Zelbig, M.; Öse, W.; Standfuss, D.; Kirk, H.; Hesse, R.; Götze, H.; Unger, W. U.S. Patent 4,767,458, Aug. 30, 1998.

10.1021/ic061765w CCC: $37.00
Published on Web 01/12/2007

fluorides and metal phosphates, metal fluoride/metal phosphate fluxes, conversion of the readily soluble $(NH_4)_2PO_3F$ with metal salts in aqueous solutions, and neutralization of metal salts with free monofluorophosphoric acid, H_2PO_3F, which can be obtained from $(NH_4)_2PO_3F$ in an ion-exchange column. Disadvantages of these reactions are the frequently observed multiphase formation when employing thermal methods and the hydrolysis of the fluorophosphate anion to phosphate and fluoride when working in aqueous solutions. A more convenient method makes use of the metathesis reaction of the reasonably soluble silver salt Ag_2PO_3F and corresponding metal chlorides in aqueous solutions: $Ag_2PO_3F + 2M^ICl/(M^{II}Cl_2) \rightarrow M^I{}_2PO_3F/(M^{II}PO_3F) + 2AgCl(\downarrow)$.[1] Along with the silver chloride, phosphates, as possible hydrolysis products, are simultaneously precipitated as Ag_3PO_4, and crystallization from the remaining filtrate leads to single-phase products.

Although the preparation of Ag_2PO_3F was described nearly 80 years ago,[7] no details on its crystal structure or other physical properties are known so far, which motivated us to reinvestigate this compound with different modern analytical methods. In this work, the synthesis and characterization of Ag_2PO_3F by single-crystal X-ray diffraction, thermal analysis, vibrational spectroscopy, and solid-state NMR spectroscopy are reported.

Experimental Section

Preparation. All reagents used were of analytical grade. Polycrystalline $(NH_4)_2PO_3F$ was synthesized according to ref 8 from stoichiometric mixtures of $(NH_4)_2HPO_4$ and $NH_4F{\cdot}HF$ in a urea melt at 170 °C for 2 h. The product was then recrystallized from an acetone/water solution. X-ray powder diffraction (XRPD) revealed a single-phase product.

The following procedure for the preparation of microcrystalline Ag_2PO_3F was carried out at room temperature: 3.2×10^{-2} mol of $(NH_4)_2PO_3F$ was dissolved in 10 mL of demineralized water, and a diluted $AgNO_3$ solution was added to separate the phosphate anions which were present in the solution because of the hydrolysis of the monofluorophosphate anion; this resulted in an immediate precipitation of yellow Ag_3PO_4. The addition of the $AgNO_3$ solution was repeated until the resulting precipitate had a white color, indicating the formation of Ag_2PO_3F. Then the precipitates were filtered off, and 8×10^{-2} mol of coarse crystalline $AgNO_3$ was added to the clear filtrate. The suspension was filled up to a volume of 250 mL with demineralized water under constant stirring for half an hour. The precipitated Ag_2PO_3F was then separated by filtration; additional material was obtained by adding 100 mL of ethanol to the remaining filtrate. The combined white Ag_2PO_3F precipitates were finally dried in a desiccator over $CaCl_2$ for 2 days. The purity of the product was checked by XRPD. The material is stable under normal atmospheric conditions but darkens slowly when exposed to daylight.

Ag_2PO_3F single crystals suitable for conventional X-ray structure analysis were grown from a diluted Ag_2PO_3F solution (300 mg Ag_2PO_3F dissolved in 20 mL of demineralized water) by slow evaporation of the solvent at room temperature in the dark. After one week, colorless crystals with mostly platelike habit up to 0.8 mm in length had formed in the remaining solution. They were separated by filtration and washed with ethanol, acetone, and diethylether.

Single-Crystal Diffraction Intensities. Single-crystal diffraction intensities were collected at 22(1) °C on a SMART three-circle diffractometer (Siemens) equipped with an APEX CCD camera (Bruker-AXS), using Mo K$\bar{\alpha}$ radiation (0.71073 Å) and the ω-scan technique with a 0.3° rotation width and 20 s exposure per frame. Three independent sets of 600 frames were recorded, thus scanning the whole reciprocal sphere. The measured intensities were corrected for Lorentz and polarization effects, and an absorption correction was applied using the multiscan approach with the program SADABS.[9] The crystal structure of Ag_2PO_3F was solved by direct methods and refined with the SHELXTL program package.[10] In the final refinement cycles, the temperature factors of all atoms were refined anisotropically, and the final difference Fourier maps did not indicate any additional atomic sites. The highest difference peaks were located close to the silver positions. Crystal data of this new compound were standardized with the program STRUCTURE-TIDY.[11] Further details of the data collection and refinement are summarized in Table 1; atomic parameters and isotropic displacement parameters are given in Table 2, and selected distances and angles as well as bond-valence sums (BVS)[12] for the individual atoms, calculated with the parameters of Brese and O'Keeffee,[13] are listed in Table 3. Drawings of structural details were produced using the program ATOMS.[14]

Vibrational Spectra. The infrared spectra were recorded as Nujol mulls between KBr plates in the spectral range between 4000 and 500 cm^{-1} employing a Bruker EQUINOX-55 FTIR instrument. Changes in band position and intensities with time could be observed using KBr disks in the usual way. This is a well-known behavior for silver salts which originates from interchange processes that occur in the alkali halide matrix.[15] Raman spectra were obtained using the FRA 106 Raman accessory of a Bruker IFS 66 FTIR spectrophotometer. The samples were excited employing the 1064 nm line of a solid-state Nd:YAG laser. The spectral resolution was $\pm$ 4 cm^{-1} in both measurements.

Thermal Analysis. Both thermogravimetry (TG) and differential scanning calorimetry (DSC) of Ag_2PO_3F were performed with a heating rate of 10 °C/min in a flowing nitrogen atmosphere. The NETZSCH TG 209 F1 IRIS (TG, aluminum oxide crucibles) and

(4) (a) Duprat, M.; Lafont, M. C.; Moran, F.; Rocher, S. *Rev. Fr. Sci. Eau* **1985**, *4*, 1−15. (b) Durand, J.; Larbot, A.; Cot, L.; Duprat, M.; Dabosi, F. *Z. Anorg. Allg. Chem.* **1983**, *504*, 163−72. (c) Laamari, M. R.; Derja, A.; Benzakour, J.; Berraho, M. *Ann. Chim.* **2001**, *26*, 117−130. (d) Laamari, M. R.; Derja, A.; Benzakour, J.; Berraho, M. *J. Electroanal. Chem.* **2004**, *569*, 1−6. (e) Chaussadent, T.; Nobel-Pujol, V.; Farcas, F.; Mabille, I.; Fiaud, C. *Cem. Concr. Res.* **2006**, *36*, 556−561.

(5) Boffardi, B. P.; Sherbondy, A. M. European Patent (EP) 481,669, April 22, 1992.

(6) (a) Lioté, F.; Bardin, C.; Liou, A.; Brouard, A.; Terrier, J.-L.; Kuntz, D. *Calcif. Tissue Int.* **1992**, *50*, 209−13. (b) Ringe, J. D.; Kipshoven, C.; Coster, A.; Umbach, R. *Osteoporosis Int.* **1999**, *9*, 171−178. (c) Duff, E. J. *Caries Res.* **1983**, *17* (Suppl 1), 77−87. (d) Root, M. J.; Schreiber, R. S. *Caries Res.* **1990**, *24*, 30−2. (e) Bruun, C.; Givskov, H. *Caries Res.* **1993**, *27*, 96−99. (f) Billington, R. W.; Williams, J. A.; Dorban, A.; Pearson, G. J. *Biomaterials* **2004**, *25*, 3399−3402.

(7) Lange, W. *Ber. Dtsch. Chem. Ges.* **1929**, *62B*, 793−801.

(8) Schülke, U.; Kayser, R. *Z. Anorg. Allg. Chem.* **1991**, *600*, 221−226.

(9) Sheldrick, G. M. *SADABS*; University of Göttingen: Göttingen, Germany.

(10) Sheldrick, G. M. *SHELXTL*, version 6.14; Bruker AXS Inc.: Madison, WI.

(11) Gelato, L. M.; Parthé, E. *J. Appl. Crystallogr.* **1987**, *20*, 139−143.

(12) Brown, I. D. *The Chemical Bond in Inorganic Chemistry*; Oxford University Press: Oxford, U.K., 2002.

(13) Brese, N. E.; O'Keeffe, M. *Acta Crystallogr.* **1991**, *B47*, 192−197.

(14) Dowty, E. *ATOMS for Windows*, version 6.2; Shape Software: Kingsport, TN, 2001.

(15) Baran, E. J.; Aymonino, P. J. *Spectrochim. Acta* **1968**, *24A*, 288−291.

Table 1. Details of Data Collection, Structure Solutions, and Refinement for Ag_2PO_3F

formula weight (g mol^{-1})	313.71
space group	*C2/c* (No. 15)
crystal dimensions (mm)	0.30 × 0.10 × 0.01
crystal description	colorless plate
Z	8
a (Å)	9.2456(8)
b (Å)	5.5854(5)
c (Å)	14.7840(13)
β (deg)	90.178(2)
vol (Å^3)	763.45(12)
μ (mm^{-1})	10.562
X-ray density (g cm^{-3})	5.459
$\theta_{min}-\theta_{max}$ (deg)	2.76−30.50
h, *k*, *l* range	$-13 \le h \le 13$, $-7 \le k \le 6$, $-21 \le l \le 21$
measured reflections	4176
independent reflections	1165
observed reflections [$I > 2\sigma(I)$]	1093
R_i	0.028
coefficients of transmission T_{min}, T_{max}	0.1438, 0.9017
parameters	67
extinction coefficient (SHELXL97)	0.00095(11)
difference electron density (e Å^{-3})	$\Delta\rho_{max} = 0.93$ (0.91, Ag1)
with distance to atom (Å)	$\Delta\rho_{min} = -0.83$ (0.95, P)
R[$F^2 > 2\sigma(F^2)$]	0.0268
wR(F^2 all)	0.0665
Goodness of fit	1.133
CSD number	416858

Table 2. Atomic Coordinates and Equivalent Isotropic Displacement Parameters (Å^2) for Ag_2PO_3F

atom	Wyckoff position	*x*	*y*	*z*	U_{eq}[a]
Ag1	8*f*	0.34945(4)	0.03649(6)	0.33469(2)	0.03017(12)
Ag2	4*e*	0	0.03118(7)	1/4	0.02636(13)
Ag3	4*a*	0	0	0	0.02925(13)
P	8*f*	0.31271(10)	0.04288(15)	0.11918(6)	0.01827(18)
O1	8*f*	0.4265(3)	0.2335(5)	0.13305(17)	0.0263(5)
O2	8*f*	0.1606(3)	0.1393(5)	0.10971(18)	0.0273(5)
O3	8*f*	0.1755(3)	0.3362(5)	0.31570(18)	0.0294(6)
F	8*f*	0.3483(3)	0.0700(5)	0.52419(16)	0.0330(5)

[a] $U_{eq} = (1/3)\sum_i\sum_j U_{ij} a_i^* a_j^* \mathbf{a}_i \mathbf{a}_j$.

the NETZSCH DSC 204 F1 (DSC, aluminum pans with pierced lid) were employed. In complementary experiments, the thermal behavior was further investigated by means of simultaneous thermal analysis coupled with Fourier transform infrared spectroscopy (BRUKER FTIR TENSOR) and with mass spectrometry (STA-FTIR−MS) measurements.

NMR Spectroscopy. Solid-state ^{31}P and ^{19}F MAS NMR experiments were performed on a Varian INOVA-300 spectrometer (7.05 T), using a home-built 5 mm, 5-turn X-{^{1}H/^{19}F} CP/MAS probe employing transmission-line tuning[16] for the high-frequency ^{1}H/^{19}F channel. Heteronuclear, high-power ^{31}P{^{19}F} and ^{19}F{^{31}P} decoupling experiments were performed, employing the WALTZ-16 decoupling scheme for rf field strengths of $\gamma B_2/2\pi = 105$ kHz and $\gamma B_2/2\pi = 50$ kHz, respectively, to reduce the ^{31}P−^{19}F couplings. The ^{31}P MAS NMR spectra were acquired at a resonance frequency of $\nu_L = 121.422$ MHz, using a ∼30° pulse ($\tau_p = 2.0$ μs for $\gamma B_1/2\pi = 40$ kHz), while the ^{19}F MAS NMR spectra ($\nu_L = 282.210$ MHz) employed a ∼75° pulse ($\tau_p = 2.0$ μs for $\gamma B_1/2\pi = 105$ kHz). The ^{19}F and ^{31}P isotropic chemical shifts are referenced to neat $CFCl_3$ and 85% H_3PO_4, respectively.

The ^{109}Ag MAS NMR spectrum ($\nu_L = 18.608$ MHz) was obtained on a Varian INOVA-400 spectrometer (9.39 T), using a home-built MAS probe for 7 mm o.d. rotors. To reduce effects from acoustic ringing, the spectrum was recorded using a Hahn-echo sequence (90° − τ − 180° − τ) with a 90° pulse of 9.5 μs and an echo delay of $\tau = 240$ μs, corresponding to one rotor period ($\nu_R = 4160$ Hz). The ^{109}Ag chemical shifts are referenced to the resonance of a 9 M silver nitrate solution which includes 0.25 M $Fe(NO_3)_2$ to enhance the efficiency of T_1 relaxation.

Simulations, least-squares fitting, and error analysis of the experimental spectra were performed using the *STARS* program package.[17] The chemical shift anisotropy (CSA) parameters are defined as $\delta_{iso} = 1/3(\delta_{xx} + \delta_{yy} + \delta_{zz})$, $\delta_\sigma = \delta_{iso} - \delta_{zz}$, and $\eta_\sigma = (\delta_{xx} - \delta_{yy})/\delta_o$, using the convention $|\delta_{zz} - \delta_{iso}| \ge |\delta_{xx} - \delta_{iso}| \ge |\delta_{yy} - \delta_{iso}|$.

Table 3. Selected Interatomic Distances (Å), Angles (deg), and Bond Valence Sums (BVS, vu)[a]

Ag1−O3	2.338(3)	Ag3−O2	2.329(3)
Ag1−O2#1	2.368(3)	Ag3−O2#5	2.329(3)
Ag1−O1#2	2.392(3)	Ag3−O1#6	2.560(3)
Ag1−O3#1	2.499(3)	Ag3−O1#3	2.560(3)
Ag1−F	2.808(3)	Ag3−F#7	2.805(3)
Ag1−O1#1	3.100(3)	Ag3−F#1	2.805(3)
Ag2−O1#1	2.492(3)	P−O3#1	1.507(3)
Ag2−O1#3	2.492(3)	P−O1	1.510(3)
Ag2−O3	2.543(3)	P−O2	1.512(3)
Ag2−O3#4	2.543(3)	P−F#8	1.575(2)
Ag2−O2	2.625(3)		
Ag2−O2#4	2.625(3)		
O3#1−P−O1	113.84(15)	O3#1−P−F#8	104.36(16)
O3#1−P−O2	113.41(16)	O1−P−F#8	104.83(14)
O1−P−O2	114.14(15)	O2−P−F#8	104.89(15)
Ag1	0.98	Ag2	0.89
Ag3	0.90	P	5.14
O1	1.92	O2	1.96
O3	1.93	F	1.20

[a] Symmetry transformations used to generate equivalent atoms: #1 1/2 − *x*, *y* − 1/2, 1/2 − *z*; #2 1 − *x*, *y*, 1/2 − *z*; #3 *x* − 1/2, *y* − 1/2, *z*; #4 −*x*, *y*, 1/2 − *z*; #5 −*x*, −*y*, −*z*; #6 1/2 − *x*, 1/2 − *y*, −*z*; #7 *x* − 1/2, 1/2 − *y*, *z* − 1/2; #8 *x*, −*y*, *z* − 1/2.

Results and Discussion

Structure Description. Under the given experimental conditions, a possible hydrolysis of the monofluorophosphate ion, resulting in a replacement of the F^- ion by the OH^- ion, has to be considered. However, IR measurements of the bulk material in the range of 4200−2000 cm^{-1} did not reveal any significant incorporation of OH^- into the structure.

The unique crystal structure of Ag_2PO_3F comprises three crystallographically independent Ag^+ cations and one PO_3F^{2-} anion as the main building units. The Ag^+ cations show strongly different coordination polyhedra, with one Ag^+ in distorted tetrahedral (Ag1), one in distorted octahedral (Ag2), and one in nearly rectangular (Ag3) coordination by oxygen atoms. This varying crystal-chemical behavior of silver has frequently been observed in numerous oxoargentates and silver oxocompounds, as described in a recent review,[18] with a broad spectrum of coordination numbers, ranging from a

(16) Jakobsen, H. J.; Daugaard, P.; Hald, E.; Rice, D.; Kupce, E.; Ellis, P. D. *J. Magn. Reson.* **2002**, *156*, 152−154.

(17) Skibsted, J.; Nielsen, N. C.; Bildsøe, H.; Jakobsen, H. J. *J. Magn. Reson.* **1991**, *95*, 88−117; *Chem. Phys. Lett.* **1992**, *188*, 405−412.

(18) Müller-Buschbaum, Hk. *Z. Anorg. Allg. Chem.* **2004**, *630*, 2125−2175.

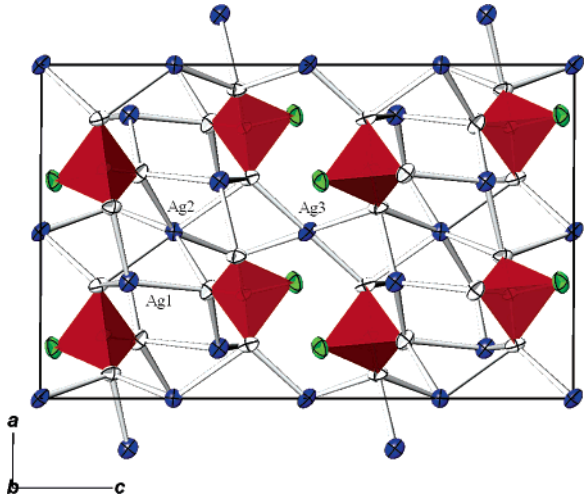

Figure 1. Crystal structure of Ag_2PO_3F in projection down [010] with the unit cell outlined and with anisotropic displacement parameters drawn at the 50% probability level. The Ag atoms are given in blue, F atoms in green, and O atoms in white; the PO_3F units are displayed as red tetrahedra.

coordination number (CN) of 3 up to 12, and with variable coordination spheres for Ag^+. The different [AgO_x] coordination polyhedra in Ag_2PO_3F are also reflected by the variations of the average Ag−O distances (viz., 2.399 Å for the tetrahedral, 2.553 Å for the octahedral, and 2.445 Å for the rectangular (square) coordination). These average values agree well with those of comparable [AgO_x] coordination polyhedra observed in the structures of other silver oxocompounds.[19] Additional weak Ag−F interactions at distances >2.80 Å (Table 3) augment the coordination polyhedra for Ag1 and Ag3, resulting in a capped tetrahedron [$Ag1O_4F$] and an axially elongated octahedron [$Ag3O_4F_2$]. Neglecting these weak Ag−F interactions (the contributions of the corresponding bond valences are only 0.04 valence units), the framework of the structure might be described as being composed of [$Ag1O_4$] and [$Ag2O_6$] polyhedra sharing edges and corners to establish silver−oxygen layers parallel to (001). These layers are joined by [$Ag3O_4$] along [001] into a three-dimensional network. The P atoms of the tetrahedral monofluorophosphate anions are situated in the cavities of the silver−oxygen network, with three bonds to oxygen atoms and one additional bond to one F atom (Figure 1). In comparison with an ideal PO_4 tetrahedron ($\bar{d}$(P−O) = 1.535 Å, ∠(O−P−O) = 109.45°), the P−O bond lengths (av 1.510 Å) are decreased, and the P−F bond length (1.575(2) Å) is increased, just like the ∠(O−P−O) angles (av 113.8°) are widened and the corresponding ∠(O−P−F) angles (av 104.7°) are reduced. This behavior has been found in most monosubstituted phosphates of the type PO_3X, where X = H, OH, OR, F and is attributed to the increasing π character per P−O bond.[20] The average values (distances and angles) of the monofluorophosphate anion in Ag_2PO_3F agree well with those found in other anhydrous monofluorophosphates, for example, in Hg_2PO_3F[21] d(P−O) = 1.515 Å, d(P−F) = 1.568(8) Å, ∠(O−P−O) = 113.0°, ∠(O−P−F) = 105.7°; in K_2PO_3F[22] d(P−O) = 1.484 Å, d(P−F) = 1.609 Å, ∠(O−P−O) = 114.4°, ∠(O−P−F) = 103.9°; in β-Na_2PO_3F[23] d(P−O) = 1.493 Å, d(P−F) = 1.606 Å, ∠(O−P−O) = 115.0°, ∠(O−P−F) = 103.1°; and in $SnPO_3F$[24] d(P−O) = 1.48 Å, d(P−F) = 1.57 Å, ∠(O−P−O) = 114.2°, ∠(O−P−F) = 104.1°. In all these monofluorophosphates, the PO_3F^{2-} anion deviates only slightly from C_{3v} symmetry. The shortest F−F distance between two PO_3F tetrahedra in Ag_2PO_3F is 2.802(5) Å which is comparable to that of 2.719 Å in β-Na_2PO_3F[23] but much shorter than the F−F distance in the mercurous compound Hg_2PO_3F (3.171(18) Å).[21]

Because the monofluorophosphate anion and the sulfate anion are isoelectronic, one might expect similar physical and chemical properties for the corresponding salts, in this case Ag_2PO_3F and Ag_2SO_4. Indeed, the solubility of Ag_2PO_3F and Ag_2SO_4 is relatively high for a silver salt, but there is no close relation between their crystal structures, despite a similar configuration of the tetrahedral $PO_3F^{2-}$and SO_4^{2-} anions.[25] Ag_2SO_4 adopts the thenardite structure type[26] and crystallizes in the orthorhombic space group *Fddd* with isolated SO_4 tetrahedra and six-coordinated Ag atoms in a strongly distorted trigonal prismatic environment.

Each of the three oxygen atoms in Ag_2PO_3F is coordinated by three Ag atoms and one P atom resulting in distorted [OAg_3P] tetrahedra, whereas the F atom is bonded to one P and two Ag atoms in a distorted trigonal fashion. The results of the bond-valence sum calculations for the different atoms in the asymmetric unit are in agreement with the expected formal charges of the individual elements (see Table 3).

Vibrational Spectra. On the basis of the reported structural data, it is possible to perform an analysis of the vibrational behavior of the PO_3F^{2-} anion. The obtained IR and Raman spectra are shown in Figure 2. As can be seen, both spectra are rather simple presenting only a reduced number of bands, without clear signs of splitting or unfolding. Therefore, it seems sufficient to analyze these spectra with the aid of the simple site-symmetry approximation, correlating the symmetry of the "free" PO_3F^{2-} anion (C_{3v}) with that of its site symmetry (C_1).[27−29] The result of this analysis is

(19) Weil, M. *Z. Naturforsch.* **2003**, *58b*, 1091−1096.
(20) Corbridge, D. E. C. *The Structural Chemistry of Phosphorus;* Elsevier: Amsterdam, 1974.
(21) Weil, M.; Puchberger, M.; Baran, E. J. *Inorg. Chem.* **2004**, *43*, 8330−8335.
(22) Payen, J.; Durand, J.; le Cot, L.; Galigne, J. L. *Can. J. Chem.* **1979**, *57*, 886−889.
(23) Durand, J.; le Cot, L.; Galigne, J. L. *Acta Crystallogr.* **1974**, B*30*, 1565−1569.
(24) Berndt, A. F. *Acta Crystallogr.* **1974**, *B30*, 529−530.
(25) In fact some monofluorophosphates and corresponding sulfates crystallize in the same structure type, for example, $Na_2PO_3F{\cdot}10H_2O$[25a] and $Na_2SO_4{\cdot}10H_2O$,[25b] β-K_2PO_3F[25c] and β-K_2SO_4,[25d] or $BaPO_3F$[25e] and $BaSO_4$.[25f] (a) Prescott, H. A.; Troyanov, S. I.; Kemnitz, E. *J. Solid State Chem.* **2001**, *156*, 415−421. (b) Levy, A. H.; Lisensky, G. C. *Acta Crystallogr.* **1978**, *B34*, 3502−3510. (c) Payen, J. L.; Durand, J.; Cot, L.; Galigné, J.-L. *Can. J. Chem.* **1979**, *57*, 886−889. (d) McGinnety, J. A. *Acta Crystallogr.* **1972**, *B28*, 2845−2852. (e) Bengtsson, E. *Arkiv Kemi. Mineral. Geol.* **1941**, *15b*, 8. (f) Hill, R. J. *Can. Mineral.* **1977**, *15*, 522−526.
(26) Mehrotra, B. N.; Hahn, T.; Eysel, W.; Roepke, H.; Illguth, A. *Neues Jahrb. Mineral., Monatsh.* **1978**, 408−421.
(27) Ross, S. D. *Inorganic Infrared and Raman Spectra*; McGraw Hill: London, 1972.
(28) Müller, A.; Baran, E. J.; Carter, R. O. *Struct. Bonding* **1976**, *26*, 81−139.
(29) Fadini, A.; Schnepel, F. M. *Vibrational Spectroscopy: Methods and Applications*; Ellis Horwood: Chichester, U.K., 1989.

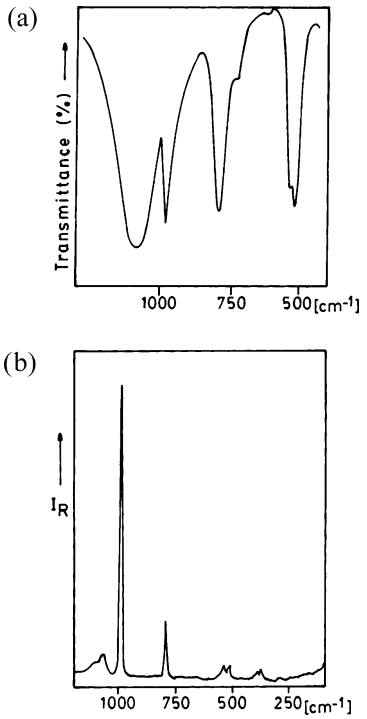

Figure 2. (a) FTIR spectrum of Ag_2PO_3F in the spectral range between 1200 and 500 cm^{-1}. (b) Raman spectrum of Ag_2PO_3F in the spectral range between 1200 and 50 cm^{-1}.

Table 4. Site Symmetry Analysis of the PO_3F^{2-} Vibrations in the Ag_2PO_3F Lattice[a]

		free anion C_{3v}	site symmetry C_1
ν_1	ν(P−F)	A_1	A
ν_2	$\nu_s(PO_3)$	A_1	A
ν_3	$\delta(FPO_3)$	A_1	A
ν_4	$\nu_{as}(PO_3)$	E	2A
ν_5	$\delta(PO_3)$	E	2A
ν_6	$\rho(PO_3)$	E	2A

[a] Space group C_{2h}^6; $Z = 8/2$. [b] Activity: A_1, E IR, Raman; A IR, Raman.

Table 5. Assignment of the IR and Raman Spectra of Ag_2PO_3F[a]

infrared[b]	Raman[b]	assignment	
1084 vs	1085sh, 1079 w	ν_4	$\nu_{as}(PO_3)$
984 s	987 vs	ν_2	$\nu_s(PO_3)$
792 vs, 727 sh	796 m	ν_1	ν(P−F)
543 sh, 519 vs	544 w, 528 w	ν_5	$\delta(PO_3)$
?	?	ν_3	$\delta(FPO_3)$
	390 w, 374 w	ν_6	$\rho(PO_3)$

[a] Band positions in cm^{-1}. [b] vs, very strong; s, strong; m, medium; w, weak; sh, shoulder.

presented in Table 4, and from these results, it becomes evident that, under site symmetry conditions, the three double-degenerated E modes are split and all vibrations remain IR and Raman active. The proposed assignments are presented in Table 5 and are briefly described as follows. (i) The ν(P−F) vibration lies at practically the same frequency as the solution value measured by Raman spectroscopy (795 cm^{-1}).[30] The respective IR band presents a weak shoulder at the lower-energy side, not predicted by the site-symmetry analysis. (ii) The $\nu_{as}(PO_3)$ vibration is extremely weak in the Raman spectrum, but it presents the two expected components. In the IR spectrum, this band is very strong and somewhat broadened. This broadening is probably generated by the superposition of the two expected components. (iii) The corresponding symmetric stretching is strong and well defined in both spectra. (iv) In the solution Raman spectrum, the ν_3 and ν_5 bands are found at the same energy (520 cm^{-1}).[30] In the present crystal spectra and following the same arguments as in the previously investigated Hg_2PO_3F,[18] we have assigned $\nu_5 > \nu_3$, on the basis of the intensity criteria, because the ν_5 vibration must be of higher intensity in the IR spectrum, as observed. On the other hand, this mode appears split in both spectra, as expected from the analysis of Table 4. The ν_3, $\delta(FPO_3)$ mode apparently does not attain enough intensity, either in the IR or in the Raman spectra, or it may lie below the measured IR range. (v) The rocking mode, ν_6, found at 379 cm^{-1} in the solution spectrum,[30] is seen as a very weak Raman doublet at 390−375 cm^{-1}.

(30) Siebert, H. *Anwendungen der Schwingungsspektroskopie in der Anorganischen Chemie*; Springer-Verlag: Berlin, 1966.

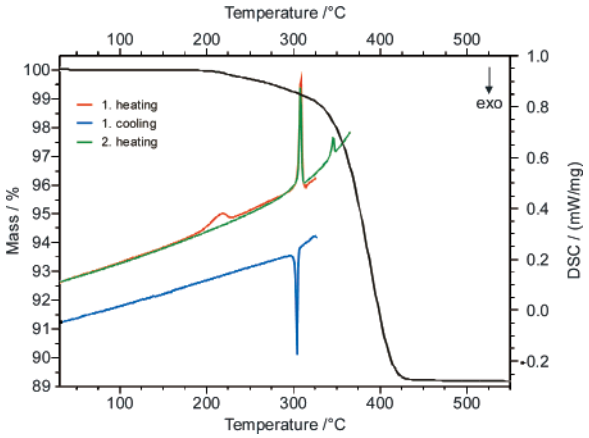

Figure 3. TG curve and DSC curves of Ag_2PO_3F.

As can be seen from Table 5, the predicted splittings of the ν_4, ν_5, and ν_6 vibrations can be observed, and the corresponding IR and Raman bands show only slight energy differences. These differences are usually considered to be a valuable criterion for the evaluation of the strength of coupling effects in the unit cell[31,32] and to confirm that these effects are relatively weak in the present lattice.

Thermal Behavior. The decomposition of the material starts with an onset of ∼200 °C (Figure 3). A small mass loss of 0.9% is observed between 200 and 325 °C, accompanied by a very small and broad irreversible endothermic DSC effect between 200 and 220 °C. The strong reversible DSC effect at 308 °C (extrapolated onset) shows a slight hysteresis and indicates the phase transition of the low-temperature (LT) Ag_2PO_3F to the high-temperature (HT) modification. Because the LT ↔ HT transition is very close to the start of the second decomposition range at ∼325 °C, a considerable amount of the material decomposes continuously when heated longer slightly above the transition point

(31) Müller, A. *Z. Naturforsch.* **1966**, *21a*, 433−436.
(32) Baran E. J.; Ferrer E. G.; Bueno I.; Parada C.; *J. Raman Spectrosc.* **1990**, *21*, 27−30.

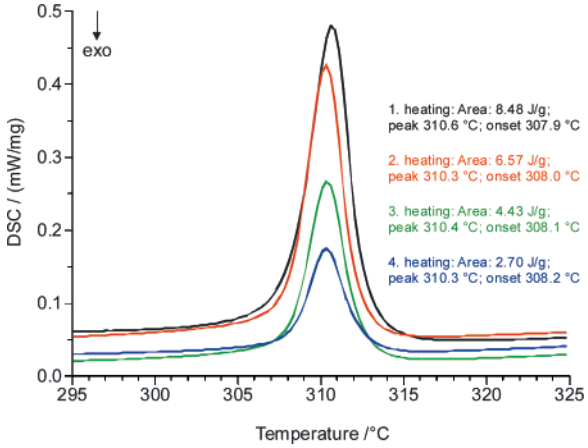

Figure 4. DSC curves of Ag_2PO_3F measured with several heating cycles between 295 and 325 °C.

or when heated and cooled in several cycles between 295 and 325 °C, as evident from the decreasing transition enthalpy in the corresponding DSC measurements (Figure 4). The pseudo-orthorhombic metrics of the LT unit cell with β close to 90° points toward a "monoclinic (LT) ↔ orthorhombic (HT)" phase transition. However, this assumption remains speculative because of the thermal instability of the high-temperature phase. From temperature-dependent XRD measurements, which were recorded slightly above the transition point (see Supporting Information), it was not possible to index the corresponding powder patterns or to derive the lattice parameters of a possible HT cell. In contrast to the relatively fast DSC measurements (duration only a few minutes), the temperature-dependent XRD measurements are too time-consuming and under these conditions the material decomposes faster than the required measuring time. Therefore, only the XRD patterns of $Ag_4P_2O_7$ and Ag_3PO_4 were observed above 310 °C. Likewise in a sample heated isothermally at 320 °C for half an hour, only minor amounts of Ag_2PO_3F were still present, whereas $Ag_4P_2O_7$ and Ag_3PO_4 were the main phases. The second strong endothermic DSC effect at 345 °C (extrapolated onset) exhibits the phase transition of $Ag_4P_2O_7$ to the high-temperature modification. Comparative DSC studies with single-phase $Ag_4P_2O_7$ are consistent (see Supporting Information) and are in very good agreement with the literature data.[33] The latter phase transition is reversible with a slight hysteresis, but no premature decomposition of $Ag_4P_2O_7$ is observed here. Qualitative phase analysis of the remaining solid obtained at 450 °C (yellow to brownish powder) revealed a phase mixture of $Ag_4P_2O_7$ and Ag_3PO_4 in an approximate ratio of 1:1; AgF melts at 435 °C[34] and is amorphous under these conditions. The theoretical mass loss of 8.29%, calculated with respect to the idealized overall reaction (eq 1), is in reasonable agreement with the experimental value of 10.8%.

$$4Ag_2PO_3F,_s \rightarrow Ag_4P_2O_7,_s + Ag_3PO_4,_s + AgF,_l + POF_3,_g\uparrow \quad (1)$$

Phosphoryl fluoride (POF_3) is the main gaseous reaction product at temperatures above 330 °C, as detected by IR and MS measurements. The recorded IR spectra (see Supporting Information) are in very good agreement with literature data,[35] and the observed molecular ion at m/z = 104, as well as other fragmentary products (see Supporting Information), matches the reference MS pattern.[36] Release of POF_3 during thermolysis of monofluorophosphates was also observed for $CaPO_3F{\cdot}2H_2O$,[37a] $SrPO_3F{\cdot}H_2O$,[37b] $Cu_2K(OH)(PO_3F)_2{\cdot}H_2O$,[37c] $BaPO_3F$,[37d] and Hg_2PO_3F.[21] In addition to POF_3, hydrogen fluoride was detected in very small amounts in the IR spectra of the gaseous decomposition products of Ag_2PO_3F at temperatures above 250 °C. This might explain the small mass loss between 200 and 300 °C and points to the presence of OH^- ions that partially replace F^- in the crystal structure. However, bands characteristic for OH^- or H_2O were not observed in the IR spectra of the employed coarse crystalline Ag_2PO_3F.

Solid-State NMR Spectra. A comparison of the ^{31}P MAS NMR spectra of Ag_2PO_3F without and with ^{19}F decoupling (Figure 5a and b) reveals a significant spectral simplification and line-narrowing of the resonances by employing high-power ^{19}F decoupling. The $^{31}P\{^{19}F\}$ MAS NMR spectrum (Figure 5b) shows the characteristic features of a manifold of spinning sidebands (ssbs) from the chemical-shift anisotropy (CSA) interaction for a single ^{31}P site, in accordance with the crystal structure. Least-squares analysis of the ssb intensities results in the parameters $\delta_{iso} = 12.7 \pm 0.2$ ppm, $\delta_\sigma = -91.6 \pm 0.7$ ppm, and $\eta_\sigma = 0.19 \pm 0.02$ and the optimized simulation of the ^{31}P CSA pattern shown in Figure 5c. Generally, isolated PO_4 tetrahedra, the so-called Q^0 groups, exhibit small CSAs as a result of their high symmetries reflected by nearly identical P−O bond lengths.[38] Thus, the large shift anisotropy ($\delta_\sigma = -91.6$ ppm) for Ag_2PO_3F reflects the coordination of phosphorus to three oxygen atoms and one fluorine atom, while the negative sign for δ_σ reflects that the P−F bond length is longer than the three P−O bonds of the PO_3F tetrahedron, following earlier studies of pyrophosphate units including one long and three short P−O bonds.[39a−c] The small value for η_σ reflects the approximate local C_{3v} symmetry of the fluorophosphate tetrahedron, where ideal C_{3v} symmetry would imply $\eta_\sigma = 0$. The ^{31}P MAS NMR spectrum (Figure 5a) includes primarily effects from the scalar $^{19}F-^{13}P$ spin−spin coupling, as reflected by the splitting of the resonances into two peaks, but it also includes effects from the magnitudes and relative orientation of the ^{31}P CSA tensor and the heteronuclear $^{19}F-^{13}P$ dipolar coupling tensor, as described earlier for static-

(33) Yamada, T; Koizumi, H; *J. Cryst. Growth* **1983**, *64*, 558−562.
(34) *CRC Handbook of Chemistry and Physics*, 76th ed., CRC Press: Boca Raton, FL, 1995.
(35) Allaf, A. W. *Spectrochim. Acta* **1998**, *A54*, 921−926.
(36) http://webbook.nist.gov/chemistry.
(37) (a) Heide, K.; Menz, D. H.; Schmidt, C.; Kolditz, L. *Z. Anorg. Allg. Chem.* **1985**, *520*, 32−38. (b) Menz, D. H.; Heide, K.; Kunert, C.; Mensing, C.; Kolditz, L. *Z. Anorg. Allg. Chem.* **1986**, *540*, 191−197. (c) Möwius, F.; Ziemer, B.; Reck, G.; Meisel, M.; Grunze, H. *Z. Anorg. Allg. Chem.* **1987**, *547*, 75−82. (d) Jäger, C.; Ehrt, D.; Haubenreisser, U. *Z. Phys. Chem.* **1988**, *159*, 75−87.
(38) Turner, G. L.; Smith, K. A.; Kirkpatrick, R. J.; Oldfield, E. *J. Magn. Reson.* **1986**, *70*, 408−415.
(39) (a) Duncan, T. M.; Douglass, D. C. *Chem. Phys.* **1984**, *87*, 339−349. (b) Hartmann, P.; Vogel, J.; Schnabel, B. *J. Magn. Reson., Ser. A* **1994**, *111*, 110−114. (c) Fyfe, C. A.; Meyer zu Altenschildesche, H.; Skibsted, J. *Inorg. Chem.* **1999**, *38*, 84−92.

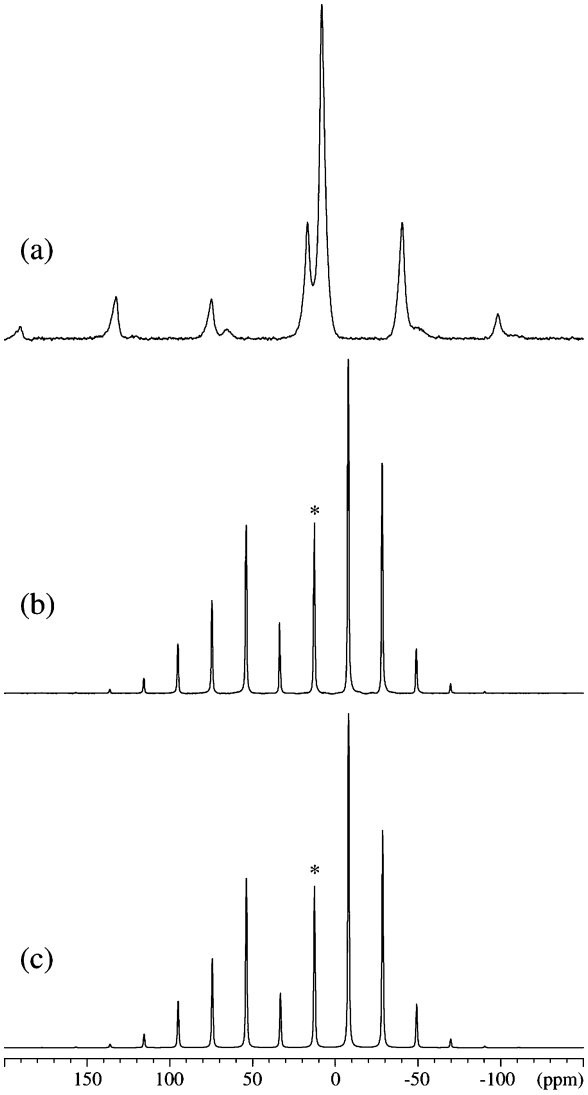

Figure 5. ^{31}P MAS NMR spectra of Ag_2PO_3F obtained (a) without and (b) with ^{19}F decoupling. The spectrum in a employed the spinning speed $\nu_R = 7.0$ kHz, a 60 s relaxation delay, and 44 scans, while $\nu_R = 2.5$ kHz, a relaxation delay of 60 s and 1156 scans were used for the ^{19}F-decoupled spectrum shown in b. (c) Simulation of the spectrum in b, corresponding to the optimized ^{31}P CSA parameters $\delta_{iso} = 12.7$ ppm, $\delta_\sigma = -91.6$ ppm, and $\eta_\sigma = 0.19$. The asterisks indicate the isotropic peak.

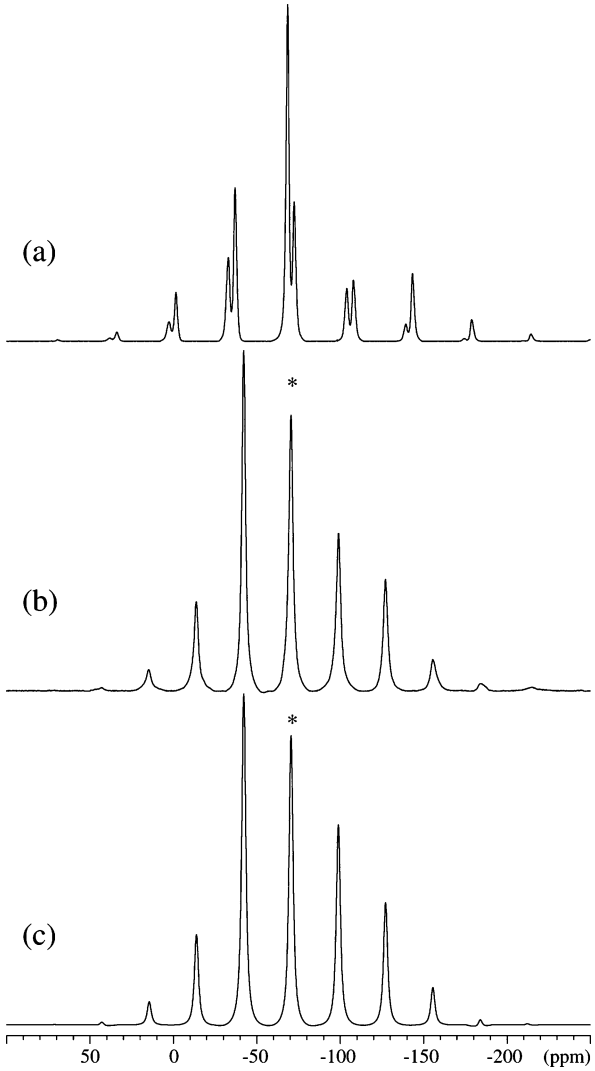

Figure 6. ^{19}F MAS NMR spectra of Ag_2PO_3F obtained (a) without and (b) with ^{31}P decoupling. The spectrum in a was obtained with a spinning speed of $\nu_R = 10.0$ kHz, a 120 s relaxation delay, and 52 scans, while $\nu_R = 8.0$ kHz, a relaxation delay of 120 s, and 43 scans were used for the spectrum shown in b. (c) Optimized simulation of the spinning sideband intensities in b, corresponding to the ^{19}F CSA parameters $\delta_{iso} = -70.6$ ppm, $\delta_\sigma = 85.6$ ppm, and $\eta_\sigma = 0.63$. The asterisks indicate the isotropic peak.

powder ^{31}P NMR experiments on fluorophosphates.[40] The splitting of the resonances in Figure 5a gives the scalar spin−spin coupling constant, $^1J_{PF} = -1045 \pm 20$ Hz, which is on the same order of magnitude as the $^1J_{PF}$ couplings reported earlier from solid-state and solution NMR studies of other monofluorophosphates.[41a−g] These data have shown a negative sign for $^1J_{PF}$ and magnitudes in the range of 500−1500 Hz.

The ^{19}F MAS NMR spectra of Ag_2PO_3F without and with ^{31}P decoupling (Figure 6a and b) exhibit the same spectral features as observed for ^{31}P and demonstrate the presence of a single ^{19}F site in the asymmetric unit. Least-squares analysis of the ssb intensities in the $^{19}F\{^{31}P\}$ MAS NMR spectrum gives the ^{19}F CSA data $\delta_{iso} = -70.6 \pm 0.3$ ppm, $\delta_\sigma = 85.6 \pm 2.2$ ppm, and $\eta_\sigma = 0.63 \pm 0.09$, corresponding to the optimized simulation in Figure 6c. The large value for η_σ indicates that the CSA tensor is significantly affected by the interactions of the fluorine atoms with neighboring silver ions.

The ^{109}Ag MAS NMR spectrum (Figure 7) shows three resonances at 190, 38, and −10 ppm in an approximate 2:1:1 ratio. On the basis of the relative intensities, the signal at 190 ppm can be assigned to the distorted tetrahedral (pentacoordinated) Ag1 site, since the crystal structure data imply a 2:1:1 ratio for the Ag1, Ag2, and Ag3 sites,

(40) Haubenreisser, U.; Sternberg, U.; Grimmer, A.-R. *Mol. Phys.* **1987**, *60*, 151−163.

(41) (a) VanderHart, D. L.; Gutowsky, H. S.; Farrar, T. C. *J. Chem. Phys.* **1969**, *50*, 1058−1065. (b) Grimmer, A. R.; Müller, D.; Neels, J. *Z. Chem.* **1983**, *23*, 140−142. (c) Grimmer, A. R.; Jost, K. H.; Müller, D.; Neels, J. *J. Fluorine Chem.* **1987**, *34*, 347−360. (d) Farrar, T. C.; Jablonsky, M. J. *J. Phys. Chem.* **1991**, *95*, 9159−9166. (e) Farrar, T. C.; Trudeau, J. D. *NATO Sci. Ser., Ser. C* **1993**, *386*, 27−48. (f) Farrar, T. C.; Schwartz, J. L.; Rodríguez, S. *J. Phys. Chem.* **1993**, *97*, 7201−7207. (g) Prescott, H. A.; Troyanov, S. I.; Kemnitz, E. *Z. Kristallogr.* **2000**, *215*, 240−245.

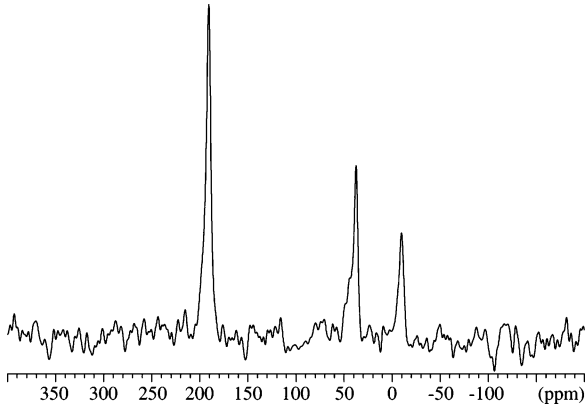

Figure 7. ^{109}Ag MAS NMR spectrum of Ag_2PO_3F recorded with the spin−echo sequence, using the spinning speed $\nu_R = 4160$ Hz, a relaxation delay of 600 s, and 596 scans.

respectively. This assignment is also consistent with the usual trend for isotropic chemical shifts as a function of coordination number, where an increase in chemical shift reflects a decrease in the coordination number. The other two ^{109}Ag resonances cannot be assigned unambiguously at the present time. However, the ^{109}Ag chemical shifts are in the spectral range of −50 to 300 ppm expected for [AgO_x] polyhedra with Ag−O bond lengths ranging from 2.329 to 2.625 Å.[42,43]

Summary

Single crystals of anhydrous disilver(I) monofluorophosphate(V), Ag_2PO_3F, were obtained by slow evaporation of a diluted aqueous Ag_2PO_3F solution. The crystal structure was determined from single-crystal data and is made up of three independent Ag^+ cations and of PO_3F^{2-} tetrahedra as simple building units. All Ag^+ cations exhibit different coordination polyhedra that share common oxygen atoms to establish a silver−oxygen network in which the P and F atoms reside. Ag_2PO_3F shows a reversible phase transition at 308 °C that is very close to the decomposition range of the material. When heated above 450 °C, Ag_2PO_3F converts to a mixture of $Ag_4P_2O_7$ and Ag_3PO_4. The vibrational spectra (IR, Raman) were interpreted by means of a unit-cell group analysis. The results from solid-state ^{19}F, ^{31}P, and ^{109}Ag MAS NMR investigations are consistent with the crystal-structure data and reveal the scalar spin−spin coupling constant, $^1J_{PF} = -1045$ Hz, in addition to reliable values for the magnitudes of the ^{19}F and ^{31}P chemical shift tensors.

Acknowledgment. Part of this work was supported by CONICET (Argentina). E.J.B. is a member of the Research Career of this organization. Discussions with Prof. Dr. Hellmut Eckert (WWU Münster) are gratefully acknowledged. The use of the facilities at the Instrument Centre for Solid-State NMR Spectroscopy, University of Aarhus, sponsored by the Danish Natural Research Council, the Danish Technical Science Research Council, Teknologistyrelsen, Carlsbergfondet, and Direktør Ib Henriksens Fond, is acknowledged. We thank Drs. E. Irran and D. Walter (TU Berlin, Germany) for the temperature-dependent X-ray powder diffraction measurements.

Supporting Information Available: Crystallographic information file (CIF) for the structure reported herein, the mass spectrum scan at 377 °C of the gaseous decomposition products of Ag_2PO_3F, the IR spectrum of the gaseous decomposition products of Ag_2PO_3F, the temperature-dependent X-ray powder diffraction measurements of Ag_2PO_3F, and the DSC measurement of single-phase $Ag_4P_2O_7$. This material is available free of charge via the Internet at http://pubs.acs.org. Further data have been deposited with the Fachinformationszentrum Karlsruhe, D-76344 Eggenstein-Leopoldshafen (crysdata@FIZ-Karlsruhe.de) and are available by quoting this article and the deposition number listed at the end of Table 1.

IC061765W

(42) van Wuellen, L.; Vensky, S.; Hoffbauer, W.; Jansen, M. *Solid State Sci.* **2005**, *7*, 920−924.
(43) Penner, G. H.; Li, W. *Inorg. Chem.* **2004**, *43*, 5588−5597.